

LA-UR 95-1436

Los Alamos National Laboratory is operated by the University of California for the United States Department of Energy under contract W-7405-ENG-36.

TITLE:

**IN SITU ION-BEAM ANALYSIS AND MODIFICATION OF SOL-GEL
ZIRCONIA THIN FILMS**

AUTHOR(S): Timothy Edge Levine, MST-4
Ning Yu, MST-4
Padma Kodali, MST-4
Kevin C. Walter, MST-4
Michael Nastasi, MST-4
Joseph R. Tessmer, MST-10
Carl J. Maggiore, MST-10

SUBMITTED TO: James W. Mayer, Arizona State University

**Presented at the Ninth International Conference on Ion
Beam Modification of Materials, Canberra, Australia
Feb. 5-10 1995**

By acceptance of this article, the publisher recognizes that the U.S. Government retains a nonexclusive, royalty-free license to publish or reproduce the published form of this contribution, or to allow others to do so, for U.S. Government purposes.

PL. Los Alamos National Laboratory requests that the publisher identify this article as work performed under the auspices of the U.S. Department of Energy

Los Alamos

Los Alamos National Laboratory
Los Alamos, New Mexico 87545

FORM NO. 620-44
51. NO. 2629 5/81

DISSEMINATION OF THIS DOCUMENT IS UNLIMITED

MASTER

Conf. 950220 --7

1

In Situ Ion-Beam Analysis and Modification of Sol-Gel Zirconia Thin Films

T. E. Levine

Department of Materials Science and Engineering, Cornell University, Ithaca, New York 14853

N. Yu, P. Kodali, K. C. Walter, M. Nastasi, J. R. Tesmer, and C. J. Maggiore

Materials Science and Technology Division, Los Alamos National Laboratory, Los Alamos, New Mexico 87545

J. W. Mayer

Department of Chem., Bio, and Materials Engineering, Arizona State University, Tempe, Arizona 85287

Abstract

We report the investigation of ion-beam-induced densification of sol-gel zirconia thin films via *in situ* ion backscattering spectrometry. We have irradiated three regions of a sample with neon, argon, and krypton ions. For each ion species, a series of irradiation and analysis steps were performed using an interconnected 3 MV tandem accelerator. The technique offers the advantages of minimizing the variation of experimental parameters and sequentially monitoring the densification phenomenon with increasing ion dose.

Typeset using REVTEX

I. INTRODUCTION

Sol-gel processing is a desirable method of ceramic thin film deposition owing to its low cost and ability to coat almost any substrate [1]. A major drawback, however, is the high temperature (700-900°C) necessary for processing which limits the choice of substrates to those with a relatively high thermal budget.

We have shown previously that sol-gel zirconia thin films can be densified through the use of ion irradiation instead of conventional heat treatment [2,3]. Also, we have demonstrated that the observed densification arises from ion-target interactions, as opposed to beam heating effects [3]. In another study, we have assumed that the observed chemical and physical changes in the films and species loss during irradiation are coupled [4]. This allows dependence on ion beam processing parameters of the observed densification to be determined by species loss alone. In this way, we have sought to determine the prominent energy loss mode through the irradiation of various inert gases. Inert gases were chosen to minimize potential chemical interaction of the ion with the target. The range of the ion was always greater than the thickness of the sol-gel film. In that work, a series of inert ions with different masses and atomic numbers were employed to systematically vary the amount of nuclear and electronic stopping in the sol-gel films. Subsequently, the films were analyzed via *ex situ* ion backscattering spectrometry (IBS), to determine species loss. Although that study suggested that the densification process has a dependence on the electronic energy loss in the target, it suffered from sample inhomogeneity and a small data set which together proved insufficient to explore the functional dependence of ion-beam-induced densification behavior on ion dose and species.

In this paper we further investigate ion-beam-induced densification via use of a specially-designed *in situ* target chamber that allows *in situ* ion beam analysis of sol-gel zirconia thin films by an interconnected analysis beamline [5]. In a typical run a sample spot is sequentially irradiated with an inert gas ion and then analyzed. This setup offers the unique abilities to minimize variation of experimental parameters and to continuously monitor the densification

process as characterized by the IBS spectra.

Prior to densification a sol-gel zirconia thin film can be pictured as an agglomeration of weakly-branched or ramified particles such that each particle is a tangled mass of oligomers [1]. During densification the film undergoes chemical and structural changes resulting in a highly-branched oxide network that ultimately collapses, driven by the high surface energy of the porous structure, into a dense ceramic film. Further as part of the formation of the oxide network, condensation reactions cross-link the particles increasing the span of the oxide network and releasing gaseous by-products (i.e. water vapor, alcohol, hydrocarbons). It is the polymeric nature of the particles and the incipient cross-linking that permits parallels with ion irradiation of polymers to be drawn to sol-gel thin films.

The property changes of polymers under ion irradiation have been shown to depend on the ion mass and atomic number, the ion energy, and the chemistry of the target [6]. But many polymers display similar effects such as cross-linking, chain scission, and release of volatile species. In general the nuclear energy loss modes are considered responsible for atomic displacement and chain scission, whereas electronic energy loss modes are considered responsible for target ionization and cross-link formation.

The sol-gel zirconia thin films of interest initially contain five species: zirconium, oxygen, carbon, hafnium, and hydrogen. The first four species each can present a definable peak in an RBS spectrum, whereas hydrogen is not directly measurable by RBS. The energy width of the zirconium peak in an RBS spectrum in the surface energy approximation is given by :

$$\Delta E = \sum_{j=1}^5 (Nt)_j [\epsilon_0]_{Zr}^j, \quad (1)$$

where ΔE is the width at half height of the zirconium peak, $(Nt)_j$ is the areal density of species j in the film and $[\epsilon_0]_{Zr}^j$ is the stopping power factor corresponding to scattering from zirconium and stopping in species j [7].

In principle the areal density of each measurable species can be calculated from the area of its peak, and together all four areal densities with the zirconium peak energy width can

be used in Eq. (1) to solve for the areal density of hydrogen. However, the relatively small areas of the constituents other than zirconium lead to erratic curves with no clear functional dependence evident. For this reason we have chosen to use the width of the zirconium peak as an indicator of species loss.

II. EXPERIMENT

A film of sol-gel zirconia was deposited onto a [100]-oriented silicon wafer in a procedure described previously [2]. A two cm square sample was installed into the *in situ* target chamber of a 200 kV implanter with an interconnected 3 MV analysis tandem accelerator [5]. Neon, argon, and krypton were implanted in the doubly charged state at 280 keV with dose rates of 6.4, 7.4, and 7.4×10^{12} ions/cm²/s, respectively. The number of IBS spectra taken were 35, 22, and 22 for neon, argon, and krypton, respectively.

Inside the *in situ* chamber, the sample normal is parallel to the implantation beam and 60° to the analysis beam. Each IBS spectrum was collected using a 3.55 MeV He⁺ beam to a total charge of 20 μ C. The analysis beam energy was chosen to take advantage of a non-Rutherford cross-section enhancement for carbon. The implanter spot size was approximately 10 mm in diameter, inside of which fit the 3×2 mm analysis spot. The analysis beam current was 40 nA. The chamber has a base pressure of 2×10^{-4} Pa. The sample stage was cooled to -100°C during irradiation.

The energy widths were measured by approximating the zirconium peaks as rectangles and determining the half height width. The uncertainty in the energy width was taken as the appropriate combination of the uncertainties in the peak area and height as governed by Poisson statistics. Energy deposited in the film was calculated using TRIM [8].

III. RESULTS/DISCUSSION

Representative IBS spectra collected during an implantation/analysis sequence are shown in Fig. 1 to illustrate the change of the spectra with ion dose. From high to low energy, the

peaks of hafnium, zirconium, oxygen, and carbon can be seen, as indicated by the surface energy markers. The most obvious change with dose is the height and the width of the zirconium peak. Other visible effects include the advancement to higher energies of the silicon substrate edge (approximately channel 550) and the decrease in area of the oxygen peak and width of the hafnium peak with increasing dose. It is worthwhile to mention that the integrated area of the zirconium peak through all experiments remained ostensibly constant negating the loss of zirconium with irradiation.

The energy widths of the zirconium peak for the three ion species are plotted in Fig. 2. The exponential-like decay of the width with dose is evident. The exponential behavior is consistent with conventional radiation damage accumulation models [9,10] and gas evolution studies of ion-irradiated polymers [11]. Comparing the curves in Fig. 2 between ion species, the rate of decay increases with ion atomic number. Additionally, the final values of the widths are not coincident. These two observations indicate that ion-beam- induced densification is dependent on the ion species, which is consistent with our previous results.

To test the effect of the analysis beam, a fresh sample was irradiated with the same analysis beam to a total charge corresponding to 15 IBS spectra, or $300 \mu\text{C}$, which is equivalent to approximately $3 \times 10^{16} \text{ He}^+/\text{cm}^2$. The total decrease in width resulting from that test was 10%, which took place within the first few spectra. This confirms that the effect of the analysis beam is negligible.

The energy width curves shown in Fig. 2 have two distinct exponential regimes as revealed in Fig. 3 along with measurement uncertainties. The existence of two linear regimes in Fig. 3 suggests that the zirconium peak width evolution can be described by the sum of two exponential terms. In light of this we have fit the energy width curves of Fig. 2 with a function of the form:

$$\Delta E(\phi) = \Delta E_\infty + C_1 \exp(-\sigma_1 \phi) + C_2 \exp(-\sigma_2 \phi), \quad (2)$$

where ΔE is the energy width of the zirconium peak at a dose ϕ , ΔE_∞ is the saturation level, C_1 and C_2 are the pre-exponential factors, and σ_1 and σ_2 represent the target species

release cross-sections. The best fit of Eq. (2) for the data is shown in Fig. 3. While the energy width of the zirconium peak is characteristic of the species remaining in the film, the functional behavior of the loss of species should obey rate laws with similar cross-sections.

While oxygen, carbon, and hydrogen are known to be leaving the film during irradiation, the data suggests the release is dominated by two kinds of species. It is plausible that the species should leave in distinct chemical groups. This would imply that the rates of decrease of the areal density, (Nt), of those three elements may be coupled into two dominant gaseous species. Indeed Chapiro [11] observed the release of H_2 , CO , CO_2 , and CH_4 during ion irradiation of PMMA. The obvious choices for released species in the zirconia sol would be H_2O , and alcohol, ROH . Determination of these species is currently in progress. As a first step, we have examined the behavior of the cross-sections, σ_1 and σ_2 , in Eq. (2) with electronic energy deposited in the film which provides a link to the further determination of released species.

Fig. 4 shows the cross-sections, σ_1 and σ_2 , versus electronic energy deposited in the film on a log-log plot. From that plot it is seen that one of the cross-sections is approximately an order of magnitude greater than the other, thus indicating that σ_2 is characteristic of a species leaving at a much faster rate than that of σ_1 . Also both cross-sections follow a similar trend, which is roughly linear with positive slope, that is the rate of species loss increases with the electronic energy deposited in the film. Insight of the interaction may be proffered by the implied power law dependence of cross-section to electronic energy loss.

Adel et al. [12] have developed a model for the release of hydrogen from amorphous hydrogenated carbon films under ion irradiation. In that model if two carbon-hydrogen bonds are broken within a certain characteristic distance, then the two hydrogen atoms can combine to form molecular hydrogen which can be liberated from the bulk. Should the hydrogen atoms not have sufficient time to diffuse together then each ion may resume some bonding configuration. According to that model, if the probability of forming a hydrogen ion scales linearly with the electronic energy loss, then a parabolic dependence of the cross-section with electronic energy loss is formed, or a line with slope 2 on a log-log plot. We desire

to extend this thinking from formation of molecular hydrogen to formation of other molecular species characteristic of the chemistry of the sol-gel zirconia thin film. For example, a hydroxyl ion formed via ion irradiation may need to diffuse a characteristic distance to combine with a alkoxy ion or another hydroxyl ion, thereby creating an alcohol or water molecule by way of a condensation reaction.

The curves of Fig. 4 have approximate slopes of 3 and 4 for σ_1 and σ_2 , respectively, suggesting that more than two free radicals combine to form a gaseous molecule, or that a modification to the model of Adel needs to be made. Perhaps the inclusion of crystallization effects may better explain the observations.

If the film crystallizes under irradiation prior to completion of chemical reactions, then further reactions would be impeded by the immobility of species in the crystalline lattice compared to the less dense porous structure. This is comparable to the competition between densification and crystallization during heat treatment of titania sol-gel films as seen by Keddie and Giannelis [13]. Titania films that were heat treated in such a way as to delay the onset of crystallization, by rapid thermal annealing for example, were found to undergo greater species loss and chemical changes than those for which the onset of crystallization occurred sooner. Greater heating rates corresponded to denser films. Ion implantation might be considered as a very rapid heating technique in this regard. Not that the temperature of the sample rises considerably during irradiation, but that there is a region of high localized temperature surrounding the ion track, known as the thermal-spike [14]. In this way an ion that imparts more energy to the film might be comparable to a faster heating rate in the sense of the work of Keddie and Giannelis. Indeed this phenomenon may be responsible for the different final energy width values in Fig. 2. As the nuclear energy deposited in the film and thermal spike effects increase in the order Ne, Ar, Kr, it might be that more energy imparted to the film translates into greater prevalence of condensation reactions and thus species loss. Conversely, the less energy that is imparted to the film does not cause the same extent of chemical reactions and may even induce the film to crystallize before those reactions can be completed, thereby inhibiting species loss.

It appears that the effect of ion irradiation on sol-gel zirconia thin films is not as straightforward as being dominated by a single process, but rather there may be a complex interplay between electronic and nuclear modes of energy loss.

IV. CONCLUSION

We have investigated *in situ* ion-beam-induced densification of sol-gel ceramic thin films. The results indicate that not only do species leave the film during irradiation, but that they may do so as two distinct groups. Additionally, the data indicates that the role of nuclear effects, perhaps in the form of crystallization, and its interplay with densification needs to be understood more fully.

ACKNOWLEDGMENTS

TEL is supported by the Army Research Office (R. Reeber, Contract No. DAAL03-89-K-0154). Further acknowledgments are due to Caleb Evans and Mark Hollander of the Ion Beam Materials Laboratory at Los Alamos National Laboratory. This work supported in part by the U.S. Dept. of Energy.

DISCLAIMER

This report was prepared as an account of work sponsored by an agency of the United States Government. Neither the United States Government nor any agency thereof, nor any of their employees, makes any warranty, express or implied, or assumes any legal liability or responsibility for the accuracy, completeness, or usefulness of any information, apparatus, product, or process disclosed, or represents that its use would not infringe privately owned rights. Reference herein to any specific commercial product, process, or service by trade name, trademark, manufacturer, or otherwise does not necessarily constitute or imply its endorsement, recommendation, or favoring by the United States Government or any agency thereof. The views and opinions of authors expressed herein do not necessarily state or reflect those of the United States Government or any agency thereof.

REFERENCES

- [1] C. J. Brinker and G. W. Scherer, *Sol-Gel Science*, (Academic Press, New York, 1990), Ch. 13.
- [2] Timothy E. Levine, Joseph L. Keddie, Peter Revesz, James W. Mayer, and Emmanuel P. Giannelis, *J. Am. Ceram. Soc.* **76**, 1369 (1993).
- [3] Timothy E. Levine, Peter Revesz, Emmanuel P. Giannelis, and James W. Mayer, *J. Vac. Sci. Technol. B* **2**, 986 (1994).
- [4] Timothy E. Levine, Emmanuel P. Giannelis, Padma Kodali, Joseph Teisser, Michael Nastasi, and Joseph W. Mayer, *Mater. Res. Soc. Symp. Proc.* **316**, p. 99 (1994).
- [5] Ning Yu, Michael Nastasi, Timothy E. Levine, Joseph R. Teisser, Mark G. Hollander, Caleb R. Evans, and Carl J. Maggiore, *Proc., Nucl. Instrum. Methods B*, in press.
- [6] T. Venkatesan, *Nucl. Instrum. Methods*, **B7**, 461 (1985).
- [7] W. K. Chu, J. W. Mayer, M. A. Nicolet, *Backscattering Spectrometry*, (Academic Press, New York, 1978), p. 79.
- [8] J. P. Biersack, L. G. Haggmark, *Nucl. Instrum. Methods* **174**, 257 (1980); **B7**, 461 (1985).
- [9] D. Pooley, *Br. J. Appl. Phys.* **76**, 855 (1965).
- [10] J. F. Gibbons, *Proc. IEEE*, **60**, 1062 (1972).
- [11] Adolphe Chapiro, *Nucl. Instrum. Methods* **B32**, 111 (1988).
- [12] M. E. Adel, O. Amir, R. Kalish, and L. C. Feldman, *J. Appl. Phys.* **66**, 3248 (1989).
- [13] Joseph L. Keddie and Emmanuel Giannelis, *J. Am. Ceram. Soc.* **74**, 2669 (1991).
- [14] John. A. Brinkman, *J. Appl. Phys.* **25**, 961 (1954).

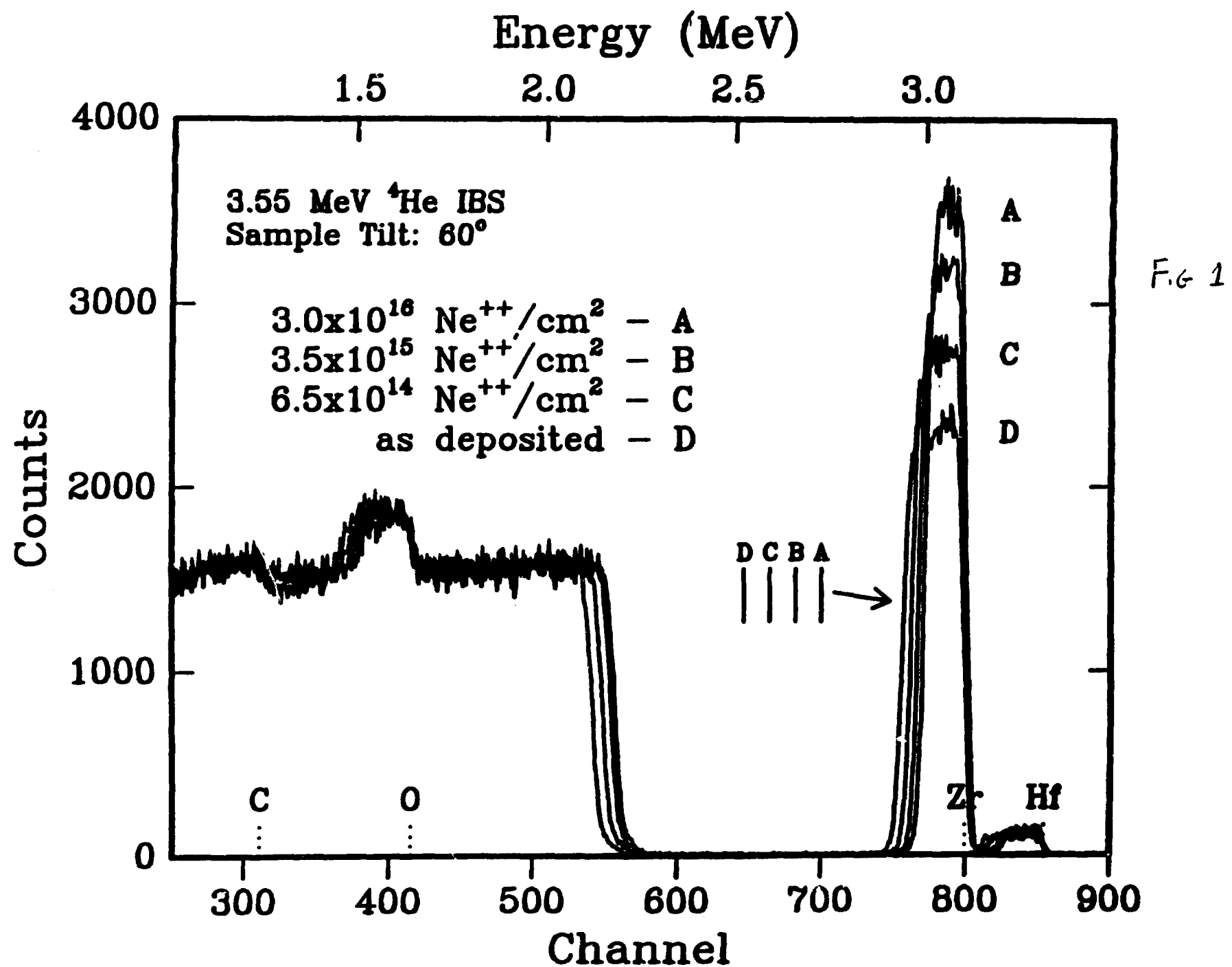
FIGURES

FIG. 1. IBS spectra of as-deposited and ion irradiated sol-gel zirconia thin film on a silicon substrate. The most notable feature is the increase in height and decrease in width of the zirconium peak, indicative of species loss. Surface energy markers indicate location of high energy edges of Hf, Zr, O, and C peaks.

FIG. 2. The zirconium peak energy width versus ion dose for three implanted species. An exponential character is evident as is the variation of the loss rate and saturation with ion species.

FIG. 3. Plot of an energy width curve with corresponding uncertainty on a semi-log plot. The broken lines guide the eye to the existence of two linear regimes. The best fit of Eq. (2) to the data is given.

FIG. 4. The cross-sections, σ_1 and σ_2 , with corresponding uncertainties plotted versus electronic energy loss. The slopes of the lines for σ_1 and σ_2 are approximately 3 and 4, respectively.



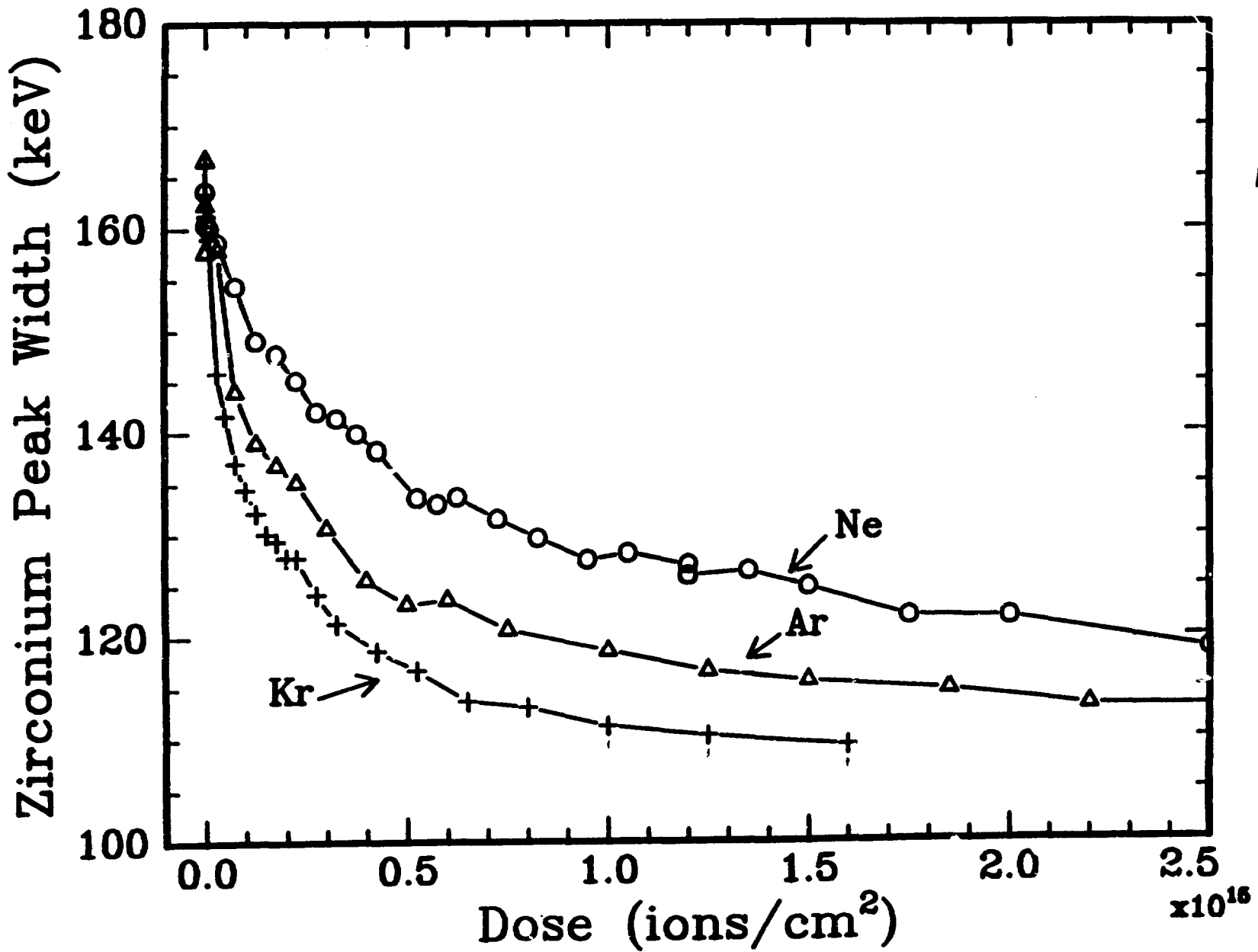


Fig. 2

